Unusual transmission bands of one-dimensional photonic crystals containing single-negative materials

Yihang Chen

Laboratory of Quantum Information Technology, School of Physics and Telecommunication Engineering, South China Normal University, Guangzhou 510006, China
kallenmail@sina.com

Abstract: Unusual transmission bands are found in one-dimensional photonic crystals composed of alternating layers of positive-index materials and single-negative (permittivity- or permeability-negative) materials. By varying the thicknesses of the positive-index material layers, the number and central frequencies of these transmission bands can be tuned. On the other hand, by varying the thicknesses of the single-negative material layers, only the bandwidths of these transmission bands will change. Furthermore, omnidirectional transmission bands for TE or TM polarization can be realized from these periodic photonic structures.

OCIS codes: (260.2110) Electromagnetic optics; (050.5298) Photonic crystals; (160.3918) Metamaterials.

References and links

1. E. Yablonovitch, "Inhibited spontaneous emission in solid-state physics and electronics," Phys. Rev. Lett. **58**(20), 2059–2062 (1987).
2. S. John, "Strong localization of photons in certain disordered dielectric superlattices," Phys. Rev. Lett. **58**(23), 2486–2489 (1987).
3. J. D. Joannopoulos, P. R. Villeneuve, and S. Fan, "Photonic crystals: Putting a new twist on light," Nature **386**(6621), 143–149 (1997).
4. P. Lodahl, A. Floris Van Driel, I. S. Nikolaev, A. Irman, K. Overgaag, D. Vanmaekelbergh, and W. L. Vos, "Controlling the dynamics of spontaneous emission from quantum dots by photonic crystals," Nature **430**(7000), 654–657 (2004).
5. S. Fan, P. R. Villeneuve, J. D. Joanopulos, and H. A. Haus, "Channel Drop Tunneling through Localized States," Phys. Rev. Lett. **80**(5), 960–963 (1998).
6. S. Noda, A. Chutinan, and M. Imada, "Trapping and emission of photons by a single defect in a photonic bandgap structure," Nature **407**(6804), 608–610 (2000).
7. Z. S. Wang, L. Wang, Y. G. Wu, L. Y. Chen, X. S. Chen, and W. Lu, "Multiple channeled phenomena in heterostructures with defects mode," Appl. Phys. Lett. **84**(10), 1629–1631 (2004).
8. Y. H. Chen, "Independent modulation of defect modes in fractal photonic crystals with multiple defect layers," J. Opt. Soc. Am. B **26**(4), 854–857 (2009).
9. J. B. Pendry, A. J. Holden, W. J. Stewart, and I. Youngs I, "Extremely low frequency plasmons in metallic mesostructures," Phys. Rev. Lett. **76**(25), 4773–4776 (1996).
10. J. B. Pendry, A. J. Holden, D. J. Robbins, and W. J. Stewart, "Magnetism from conductors and enhanced nonlinear phenomena," IEEE Trans. Microw. Theory Tech. **47**(11), 2075–2084 (1999).
11. G. S. Guan, H. T. Jiang, H. Q. Li, Y. W. Zhang, H. Chen, and S. Y. Zhu, "Tunneling modes of photonic heterostructures consisting of single-negative materials," Appl. Phys. Lett. **88**(21), 211112 (2006).
12. Y. H. Chen, J. W. Dong, and H. Z. Wang, "Twin defect modes in one-dimensional photonic crystals with a single-negative material defect," Appl. Phys. Lett. **89**(14), 141101 (2006).
13. Y. H. Chen, "Frequency response of resonance modes in heterostructures composed of single-negative materials," J. Opt. Soc. Am. B **25**(11), 1794–1799 (2008).
14. T. Fujishige, C. Caloz, and T. Itoh, "Experimental demonstration of transparency in ENG-MNG pair in a CRLH transmission-line implementation," Microw. Opt. Technol. Lett. **46**(5), 476–481 (2005).
15. L. W. Zhang, Y. W. Zhang, L. He, H. Q. Li, and H. Chen, "Experimental study of photonic crystals consisting of ε-negative and μ-negative materials," Phys. Rev. E Stat. Nonlin. Soft Matter Phys. **74**(5), 056615 (2006).
16. L. W. Zhang, Y. W. Zhang, L. He, H. Q. Li, and H. Chen, "Experimental investigation on zero-φ_{eff} gaps of photonic crystals containing single-negative materials," Eur. Phys. J. B **62**(1), 1–6 (2008).
17. H. Zhang, X. Chen, Y. Q. Li, Y. Fu, and N. Yuan, "The Bragg gap vanishing phenomena in one-dimensional photonic crystals," Opt. Express **17**(10), 7800–7806 (2009).

#115314 - $15.00 USD Received 5 Aug 2009; revised 9 Oct 2009; accepted 9 Oct 2009; published 23 Oct 2009

18. M. Centini, C. Sibilia, M. Scalora, G. D'Aguanno, M. Bertolotti, M. J. Bloemer, C. M. Bowden, and I. Nefedov, "Dispersive properties of finite, one-dimensional photonic band gap structures: applications to nonlinear quadratic interactions," Phys. Rev. E Stat. Phys. Plasmas Fluids Relat. Interdiscip. Topics **60**(4 4 Pt B), 4891–4898 (1999).
19. K. Y. Xu, X. G. Zheng, and W. L. She, "Properties of defect modes in one-dimensional photonic crystals containing a defect layer with a negative refractive index," Appl. Phys. Lett. **85**(25), 6089–6091 (2004).
20. Y. H. Chen, J. W. Dong, and H. Z. Wang, "Conditions of near-zero dispersion of defect modes in one-dimensional photonic crystals containing negative-index materials," J. Opt. Soc. Am. B **23**(4), 776–781 (2006).

1. Introduction

During the last decade, the study of electromagnetic (EM) properties of photonic crystals (PCs) has been the intriguing subject of great attention [1–4]. Conventional photonic band gap (PBG) originates from the interference of Bragg scattering in a periodical structure with positive-index materials (PIMs). Such a Bragg gap depends strongly on the details of the interference process. When the structural periodicity is broken by introducing defects into a PC, defect modes will appear inside the PBG [5,6]. One-dimensional (1D) PCs with defect layers have been used for filters that possess narrow passbands with high transmittance [7,8]. Since the defect modes originate from the interference, its frequencies will blue shift as the incident angle increases. Furthermore, the bandwidths of the passbands corresponding to the defect modes are difficult to tune. So the applications of the conventional filters are restricted.

Recently, a new type of artificial composites, in which only one of the two material parameters permittivity (ε) and permeability (μ) is negative, has been realized [9,10]. These single-negative (SNG) materials include epsilon-negative (ENG) media with negative ε but positive μ and the mu-negative (MNG) media with negative μ but positive ε. It is well known that the EM waves in the SNG materials are decaying since their wave vectors are imaginary. However, tunneling modes can be obtained in 1D photonic structures composed of alternate MNG and ENG materials [11–13]. The transmission bands corresponding to the tunneling modes are insensitive to the incident angle, but their bandwidths are still hard to control.

In this letter, 1D PCs consisting of alternating layers of PIMs and SNG (ENG or MNG) materials are demonstrated. Such PCs can produce a number of transmission bands, whose number, corresponding central frequencies and bandwidths can be controlled by changing its structural parameters. Moreover, omnidirectional transmission bands for the TE or TM wave can be realized. Such properties will lead to potential applications.

2. The model

Consider 1D PCs with the periodic structures of $(AB)^s$ and $(AC)^s$, where A represents a layer of PIM with the thickness of d_A and B (C) represents a layer of ENG (MNG) material with the thickness of d_B (d_C), and s is the number of periods. We assume that the relative permittivity and permeability take the forms of

$$\varepsilon_B = 1 - \frac{\omega_{ep}^2}{\omega^2}, \qquad \mu_B = \mu_b \tag{1}$$

in ENG materials and

$$\varepsilon_C = \varepsilon_c, \qquad \mu_C = 1 - \frac{F\omega^2}{\omega^2 - \omega_0^2} \tag{2}$$

in MNG materials, where ω_{ep} and ω_0 are, respectively, the electronic plasma frequency and the magnetic resonance frequency. These kinds of dispersion for ε_B and μ_C can be realized in special metamaterials [14–17]. In the following calculation, we choose $\mu_A = \varepsilon_A = 1$, $\mu_b = \varepsilon_c = 1$, and $\omega_{ep} = \pi c/d$, $\omega_0 = 4c/d$, $F = 0.56$.

Let a plane wave be injected from vacuum into the considered PC at an angle θ with + z direction, as show in Fig. 1. For the transverse electric (TE) [or transverse magnetic (TM)] wave, the electric field [or the magnetic field] is in the x direction. For an infinite periodic

#115314 - $15.00 USD Received 5 Aug 2009; revised 9 Oct 2009; accepted 9 Oct 2009; published 23 Oct 2009

structure $(AB)^s$ ($s \to \infty$), according to Bloch's theorem, the dispersion at any incident angle follows the relation [18]

$$\cos\beta_z(d_A+d_B)=\cos(k_{Az}d_A)\cos(k_{Bz}d_B)-\frac{1}{2}(\frac{q_A}{q_B}+\frac{q_B}{q_A})\sin(k_{Az}d_A)\sin(k_{Bz}d_B), \tag{3}$$

where β_z is the z component of Bloch wave vector, $k_{iz}=\omega/c\sqrt{\varepsilon_i}\sqrt{\mu_i}\sqrt{1-(\sin^2\theta/\varepsilon_i\mu_i)}$ (i = A, B) is the z component of the wave vector, and c is the light speed in the vacuum. For TE wave, $q_i=\sqrt{\varepsilon_i}/\sqrt{\mu_i}\sqrt{1-(\sin^2\theta/\varepsilon_i\mu_i)}$; for TM wave, $q_i=\sqrt{\mu_i}/\sqrt{\varepsilon_i}\sqrt{1-(\sin^2\theta/\varepsilon_i\mu_i)}$. The EM fields in the consider system can be propagating or evanescent, corresponding to real or imaginary Bloch wave numbers, respectively. The solution of Eq. (3) defines the band structure for the infinite system $(AB)^s$. Similarly, the dispersion relation for infinite structure $(AC)^s$ can be obtained by replacing d_B, k_{Bz} and q_B of Eq. (3) by d_C, k_{Cz} and q_C, respectively.

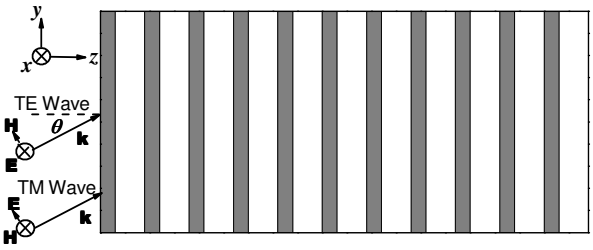

Fig. 1. Schematic representation of the PC constituted by SNG materials and PIMs. The gray and white regions represent the SNG materials and PIMs, respectively.

3. Numerical results and discussion

Firstly, we consider the infinite structure $(AB)^s$ containing ENG materials. Figure 2 shows the dependence of the band structure on the ratio of the thicknesses d_A/d_B under $d_B = d$ at normal incidence. The gray areas represent the regions of propagating states, whereas the white areas represent regions containing evanescent states. It can be seen from Fig. 2 that transmission bands appear in the ENG frequency range $0 < \omega/\omega_{ep} < 1$. As d_A increases, more and more transmission bands emerge, and these transmission bands all shift to lower frequencies. The physical mechanism of the transmission bands is different from the tunneling mechanism of the ENG-MNG multilayered periodic structure [11]. When a plane wave is incident from a PIM layer into a SNG layer, high reflection will occur at the interface. Although fields in each SNG layer are decaying, some of them can still couple into the next PIM layer. So reflected waves exist at interfaces from PIM to SNG layers. The phase difference between two neighboring reflected waves is approximate to $2k_{Az}d_A$. If the phase difference is equal to odd times of π, these reflected waves will cancel each other and thus the transmission bands form. Therefore, the frequencies of the transmission bands should be close to the values of ω satisfying

$$2k_{Az}d_A=(2t+1)\pi. \tag{4}$$

In case of normal incidence, substitute μ_A and ε_A into Eq. (4), we obtain

$$2\frac{\omega}{c}d_A=(2t+1)\pi. \tag{5}$$

For example, when $d_A = 2d$, it can be got from Eq. (5) that ω/ω_{ep} = 1/4, 3/4 corresponding to t = 0, 1. The two corresponding transmission bands exist in Fig. 2 when $d_A = 2d$, although the frequencies of them are a little different from the approximately theoretical values. For another example, when $d_A = 3d$, it can be got from Eq. (5) that ω/ω_{ep} = 1/6, 3/6, 5/6

#115314 - $15.00 USD Received 5 Aug 2009; revised 9 Oct 2009; accepted 9 Oct 2009; published 23 Oct 2009

corresponding to t = 0, 1, 2. It can be seen from Fig. 2 that the three corresponding transmission bands exist when $d_A = 3d$. Furthermore, from Eq. (5) we can obtain, as d_A increases, ω decreases and the transmission band shifts to lower frequency, in accordance with Fig. 2.

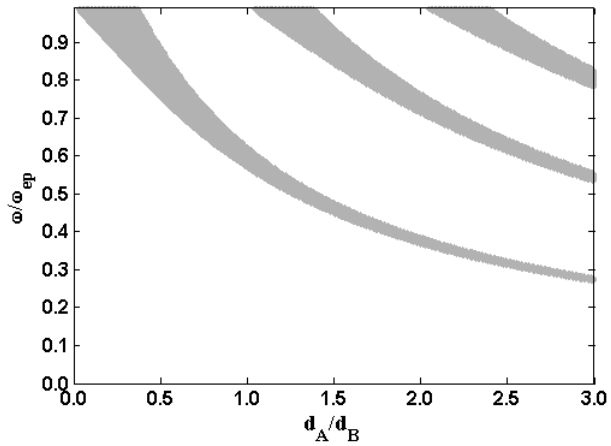

Fig. 2. Dependence of the transmission bands on the ratio d_A/d_B in infinite structure $(AB)^s$ with $d_B = d$ at normal incidence.

Next, we study the dependence of the transmission bands on the ratio d_B/d_A when d_A is fixed. In Fig. 3, we choose $d_A = 2.5d$. As shown in Fig. 3, three transmission bands appear, their central frequencies are $0.32\omega_{ep}$, $0.63\omega_{ep}$, and $0.91\omega_{ep}$, respectively. As d_B increases, the central frequencies of these bands remain invariant while the bandwidths of the transmission bands decrease. Such properties can also be understood from Eq. (5), the central frequencies of the transmission bands depend on d_A, not d_B. The properties of Figs. 2 and 3 can be used to design filters with multiple transmission channels, whose bandwidths can be varied conveniently.

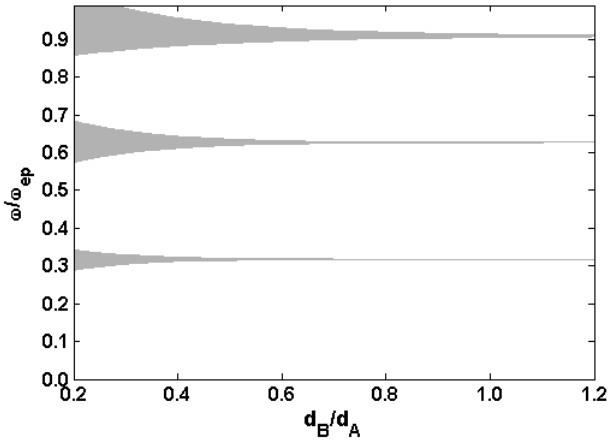

Fig. 3. Dependence of the transmission bands on the ratio d_B/d_A in infinite structure $(AB)^s$ with $d_A = 2.5d$ at normal incidence.

The dependence of the transmission spectra on d_B in finite structure $(AB)^{12}$ is shown in Fig. 4. It can be seen from Fig. 4 that the transmission bands will be narrowed with the increasing of d_B, the same as the results in Fig. 3.

#115314 - $15.00 USD Received 5 Aug 2009; revised 9 Oct 2009; accepted 9 Oct 2009; published 23 Oct 2009

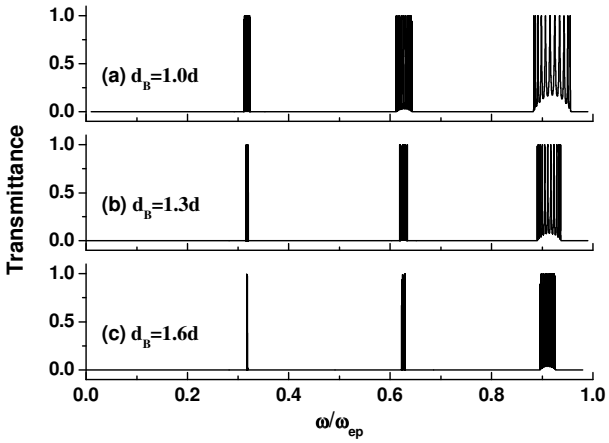

Fig. 4. Dependence of the transmission bands on d_B in finite structure $(AB)^{12}$ with $d_A = 2.5d$.

Then, we turn to investigate the dependence of the transmission bands on the incident angle. In Fig. 5 we show the dispersion relations of the transmission bands with the thicknesses $d_A = 2.5d$ and $d_B = d$. It is seen that the transmission bands are sensitive to the incident angle. The transmission bands will shift to higher frequencies as the incident angle increases. It means that the dispersion relations of such transmission bands are all positive type [19,20]. On the other hand, we note from Fig. 5 that the frequency shift of band I is relatively small for TM wave. So we then study the dependence of the dispersion relation of transmission band I on d_A, as shown in Fig. 6. It can be seen from Fig. 6(a)-6(c) that the dispersion relation of band I for TM wave changes from negative to near-zero then to positive type as d_A changes from $0.5d$ to $0.82d$ and onward to $1.5d$. As shown in Fig. 6(b), the transmission band remains almost invariant as the incident angle varies for TM wave. The transmission band with weak incident angle dependence may be useful in applications, such as omnidirectional filters.

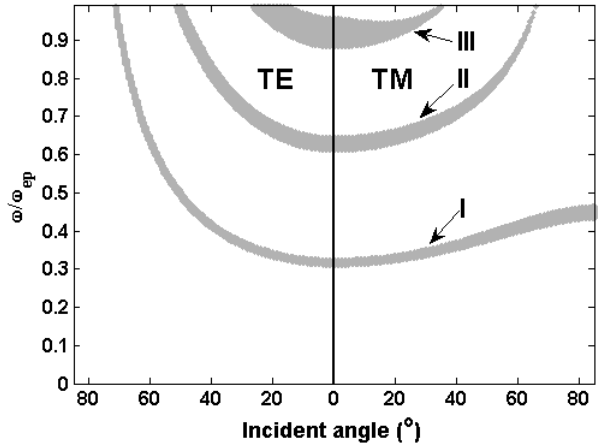

Fig. 5. Photonic band structure as a function of the incident angle in infinite structure $(AB)^s$ with $d_A = 2.5d$ and $d_B = d$.

#115314 - $15.00 USD Received 5 Aug 2009; revised 9 Oct 2009; accepted 9 Oct 2009; published 23 Oct 2009

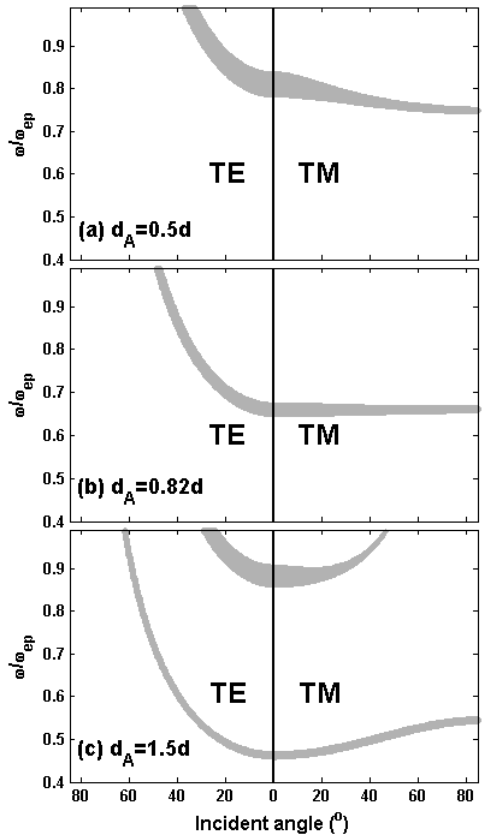

Fig. 6. Dependence of the dispersion relations of the transmission bands on d_A for infinite structure $(AB)^s$ with $d_B = 1.5d$.

Moreover, the properties of the transmission bands in structure $(AC)^s$ containing MNG materials are also studied. It is found that the properties of the transmission bands in $(AC)^s$ for TE (TM) polarization are similar to those in $(AB)^s$ for TM (TE) polarization. So the properties of the transmission bands of structure $(AC)^s$ can be easily obtained from those of $(AB)^s$.

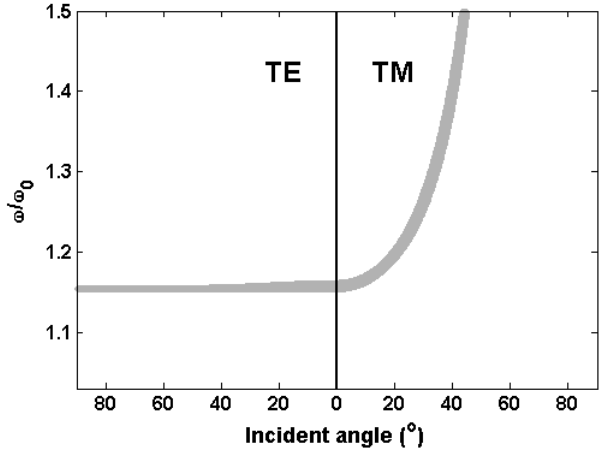

Fig. 7. Dispersion relation of the transmission band in infinite structure $(AC)^s$ with $d_A = 0.36d$ and $d_C = 0.85d$.

#115314 - $15.00 USD Received 5 Aug 2009; revised 9 Oct 2009; accepted 9 Oct 2009; published 23 Oct 2009

Figure 7 shows the dispersion relation of the transmission band in infinite structure $(AC)^s$ with $d_A = 0.36d$ and $d_C = 0.85d$. The MNG frequency range is $1 < \omega/\omega_0 < 1.5$. It is seen from Fig. 7 that the transmission band is insensitive to the incident angle for TE wave. The dependence of the transmission band on incident angle in finite structure $(AC)^{12}$ is also calculated, as shown in Fig. 8. As the incident angle θ varies, the central frequency of the transmission band remains almost invariant.

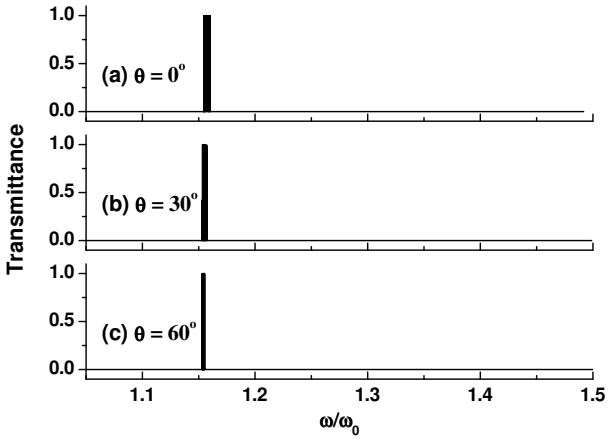

Fig. 8. Dependence of the transmission band on incident angle θ for TE wave in finite structure $(AC)^{12}$ with $d_A = 0.36d$ and $d_C = 0.85d$.

In practice, two main approaches to realize SNG materials have been reported: resonant structures made of the array of wires and split-ring resonators [9,10] and nonresonant transmission line (TL) structures made of lumped inductors and lumped capacitors [14–17]. The TL approach towards metamaterial with left-handed and right-handed attributes, known as composite right/left-handed transmission line (CRLH TL), which presents the advantage of lower losses over a broader bandwidth and has already been demonstrated in various component and coupler applications. 1D PCs containing SNG materials have been fabricated using the CRLH TL by periodically loading lumped-element series capacitors and shunt inductors [15–17]. The unit cell of the CRLH TL is shown in Fig. 9(a). The structure consists of a host TL medium with the distributed parameters L_0 and C_0 periodically loaded with discrete lumped element components, L_i and C_i. Such structure exhibits a macroscopic behavior rigorously expressed with the constitutive parameters ε and μ. The CRLH TL fabricated by cascading the unit cells of Fig. 9(a) periodically is effectively homogeneous in a certain range of frequencies [15–17]. The effective relative permittivity and permeability are given by the following approximate expressions,

$$\varepsilon_i \approx [C_0 - \frac{1}{(\omega^2 - i\gamma_e\omega)L_i d_i}]/(\varepsilon_0 p), \qquad \mu_i \approx p[L_0 - \frac{1}{(\omega^2 - i\gamma_m\omega)C_i d_i}]/\mu_0, \tag{6}$$

where p is a structure constant and $i = 1, 2$ denotes the different type of CRLH TL. γ_e and γ_m denote the respective electric and magnetic damping factors that contribute to the absorption and losses. Here we use the material parameters the same as those in Ref [15]. Consider ENG TL and PIM TL both made on a FR-4 substrate with a thickness of 1.6mm, relative permittivity $\varepsilon_r = 4.75$, and relative permeability $\mu_r = 1.0$. In this situation, $p = 4.05$. We choose $L_1 = 13$ nH, $C_1 = 8.6$ pF and $d_1 = 5$mm for the ENG TL, and $L_2 = 111$ nH, $C_2 = 8.6$ pF and $d_2 = 5$mm for the PIM TL. The calculated relative permittivity and permeability of the ENG TL and PIM TL according to Eq. (6) in the lossless case are shown in Fig. 9(b). It is clearly shown that ε and μ are dependent on the frequency. As shown in Fig. 9(b), the frequency range, where $\varepsilon<0$ and $\mu>0$, for ENG TL is 0.817-1.961 GHz, and the frequency range, where $\varepsilon>0$ and $\mu>0$, for PIM TL is over 0.817 GHz.

#115314 - $15.00 USD Received 5 Aug 2009; revised 9 Oct 2009; accepted 9 Oct 2009; published 23 Oct 2009

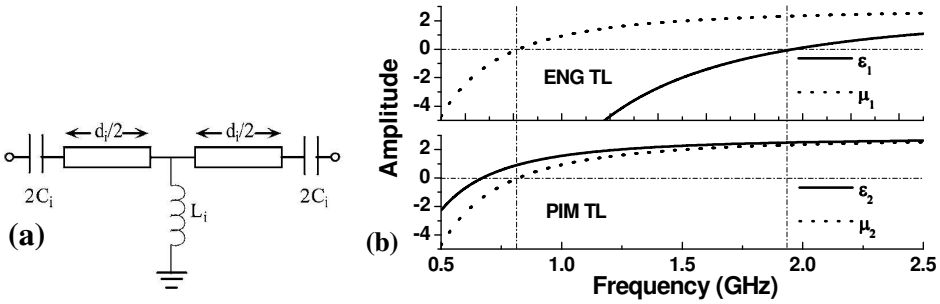

Fig. 9. (a) The schematic and circuit model of a CRLH TL unit with the loading lumped element series capacitors (C_i) and shunt inductors (L_i). (b) The calculated relative permittivity (ε) and permeability (μ) of the ENG TL and PIM TL.

In the following calculation, we use the relatively large damping factors $\gamma_e = \gamma_m = 1 \times 10^7$ Hz. Firstly, we consider the dependence of the transmission band of the $(PIM_5ENG_4)^2$ TL on the incident angle, where the subscripts "5" and "4" represent the number of PIM TL and ENG TL units in one period, respectively, and the superscript "2" represents the number of periods. As shown in Fig. 10, the central frequency of the transmission band is insensitive to the incident angle for TM wave. Such property is in accord with that of infinite structure in Fig. 6(b). The losses will only slightly decrease the transmittance.

Next, we calculate the transmission spectra of the structures $(PIM_5ENG_4)^2$, $(PIM_7ENG_4)^2$, and $(PIM_{10}ENG_4)^2$, as shown in Fig. 11(a). It is shown from Fig. 11(a) that, as the lengths of PIM TLs increase, the transmission bands shift to lower frequencies, the same as the property in Fig. 2. Figure 11(b) shows the simulated spectra of $(PIM_{10}ENG_4)^2$, $(PIM_{10}ENG_4)^3$, and $(PIM_{10}ENG_4)^4$ based on CRLH TLs. It can be seen from in Fig. 11(b) that there are $S - 1$ peaks in each transmission band in the structure $(PIM\text{-}ENG)^S$. Such properties can be explained as follows. From our previous analysis, we know that reflected wave exists at each interface from PIM to SNG layer. So there are S reflected waves exist in structure $(PIM\text{-}ENG)^S$. According to the wave optics, for S light beams with the same amplitude A_0 and phase difference $\Delta\varphi$ between two neighboring beams, if they superpose, the total amplitude is equal to $A_0[\sin(S\Delta\varphi/2)/\sin(\Delta\varphi/2)]$. From $\Delta\varphi = 0$ to 2π, the total amplitude has S-1 minimum values, corresponding to the $S - 1$ transmission peaks. For the current structure with period number S, there are S reflection beams with equal phase difference but different intensities between two neighboring beams. Although the different intensities may change the frequencies of the peaks, there still exist S–1 transmission peaks in each transmission band.

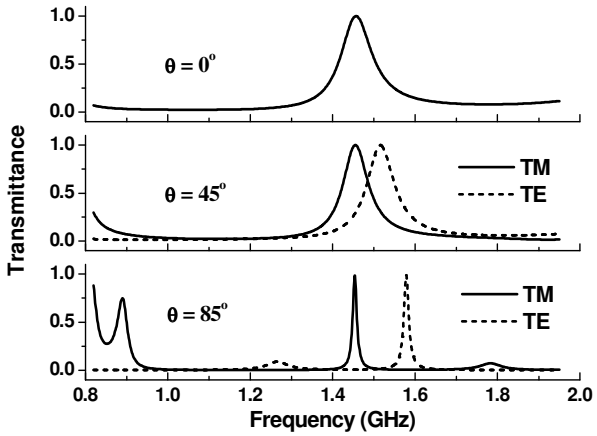

Fig. 10. Dependence of the transmission band of the $(PIM_5ENG_4)^2$ TL on the incident angle.

#115314 - $15.00 USD Received 5 Aug 2009; revised 9 Oct 2009; accepted 9 Oct 2009; published 23 Oct 2009

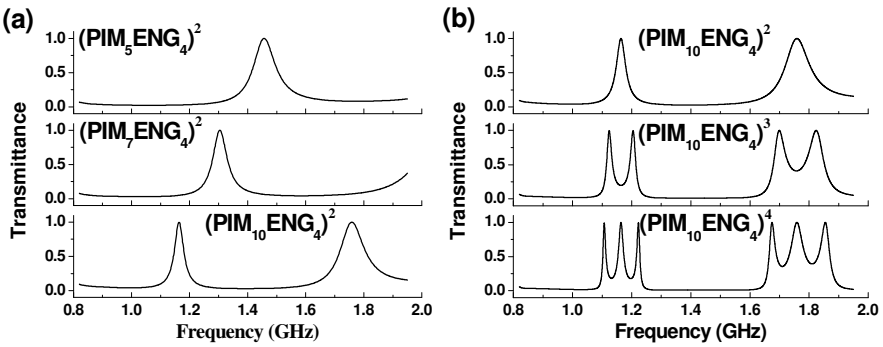

Fig. 11. (a) The simulated transmission of the structures $(PIM_5ENG_4)^2$, $(PIM_7ENG_4)^2$, and $(PIM_{10}ENG_4)^2$; (b) the simulated transmission of the structures $(PIM_{10}ENG_4)^2$, $(PIM_{10}ENG_4)^3$, and $(PIM_{10}ENG_4)^4$.

Figure 12 shows the transmission spectra of the structures $(PIM_{10}ENG_4)^4$, $(PIM_{10}ENG_5)^4$, and $(PIM_{10}ENG_6)^4$. As the lengths of ENG TLs increase, the transmission bands become narrower and narrower, while the central frequencies of the two bands are unchanged. Such result is in accordance with that of Fig. 3.

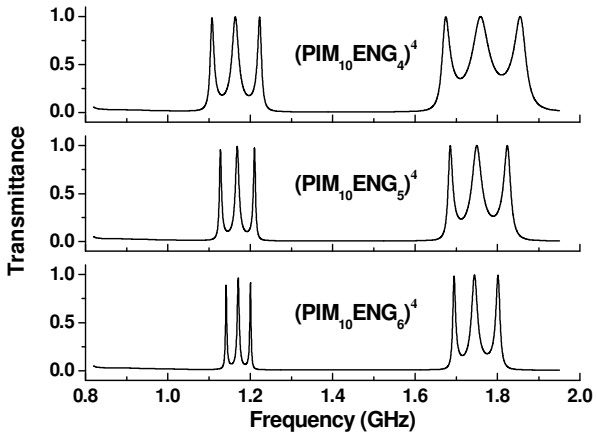

Fig. 12. The simulated transmission of the structures $(PIM_{10}ENG_4)^4$, $(PIM_{10}ENG_5)^4$, and $(PIM_{10}ENG_6)^4$.

4. Conclusion

In conclusion, we showed that 1D PCs stacking of PIMs and SNG materials can produce a number of transmission bands. The bandwidths of such transmission bands can be tuned conveniently by adjusting the thicknesses of the SNG layers. On the other hand, the number and central frequencies of these bands depend on the thicknesses of the PIM layers. Omnidirectional transmission bands for the TE or TM wave are, respectively, obtained from such PC structures containing MNG or ENG materials. Our results will lead to further applications in optical guided transmission devices, such as multichannel filters and omnidirectional filters.

Acknowledgements

This work is supported by the National Natural Science Foundation of China (Grant No. 10704027), and the Natural Science Foundation of Guangdong Province of China (Grant Nos. 9151063101000040 and 07300205).

#115314 - $15.00 USD Received 5 Aug 2009; revised 9 Oct 2009; accepted 9 Oct 2009; published 23 Oct 2009